Temperature-based diagnosis of the Gulf Stream path overestimates its northward shift in a warming ocean

Lina Garcia-Suarez[1], Katja Fennel[1], Neha Mehendale[2], Tronje Kemena[2], David P. Keller[2,3]

[1]Department of Oceanography, Dalhousie University, Halifax, NS, Canada
[2]GEOMAR Helmholtz Centre for Ocean Research Kiel, Kiel, Germany
[3]Carbon to Sea Initiative, Washington, DC, USA

Correspondence to: Lina Garcia-Suarez (lina.garcia@dal.ca)

Abstract. Temperature-based criteria for diagnosing the location of the Gulf Stream (GS) are widely used and suggest a northward shift of the GS is underway. The apparent northward shift in the GS path has been causally linked to the recent rapid warming in the northwest Atlantic Ocean. This study uses high-resolution climate models to show that temperature-based criteria for diagnosing the GS path overestimate its northward shift in warming scenarios and, for one of the models, indicate a northward shift that does not occur. In contrast, a sea surface height (SSH)-based criterion for diagnosing the GS path remains closely aligned with the true GS core in a warming ocean and thus provides a more reliable estimate of shifts in its path. The temperature-based assessments are biased by the rising background temperature in the ocean, thus creating a misleading indication of a GS migration. These results call into question the notion that warming in the northwest North Atlantic is causally related to a northward migration of the GS and emphasize the need for more robust indicators of its position.

1 Introduction

The northwest North Atlantic shelf and slope waters are undergoing some of the fastest temperature increases globally (Caesar et al., 2018; Forsyth et al., 2015; Johnson and Lyman, 2020; Williams et al., 2021), a trend projected to continue under future climate scenarios (Caesar et al., 2018; Williams et al., 2021). The rapid warming is frequently attributed to a northward migration of the Gulf Stream (Gonçalves Neto et al., 2021; Seidov et al., 2021; Todd and Ren, 2023; Wu and He, 2024). The Gulf Stream (GS) is the western boundary current of the North Atlantic subtropical gyre and transports heat from the tropics to the mid-latitudes (Palter, 2015). Changes in its strength and position significantly impact weather and climate of the eastern North Atlantic and western Europe (Ma et al., 2024; Wenta et al., 2024). However, with respect to the rapid warming of the northwest North Atlantic, observations reveal that poleward shifts in the ocean gyres, including the North Atlantic subtropical gyre, are often not statistically significant (Chi et al., 2021; Yang et al., 2016, 2020). Bisagni et al. (2017) found that between 1993 and 2013, the GS actually moved southward while Todd and Ren (2023) documented a modest northward shift using observations collected predominantly between 2015 and 2023. The lack of consistent evidence challenges the narrative that a poleward shift of the GS explains the rapid warming of the northwest North Atlantic shelves.

A widely used proxy for diagnosing the location of the GS is the North Wall, defined by the 15 ºC isotherm at 200 m (Fuglister and Voorhis, 1965). More recent studies have instead diagnosed the GS path using different isotherms, such as the 12 ºC isotherm at 450 m (Sanchez-Roman et al., 2024). These proxies, henceforth referred to as T15 and T12, are thought to be close to the maximum in GS surface current velocity. The T15 has been widely applied because long-term temperature records are available making it a convenient proxy. Many studies have assumed that changes in the North Wall, as indicated by T15, represent changes in the position of the GS, often using the two concepts interchangeably, to estimate both short- and long-term trends (Caesar et al., 2018; Hansen, 1970; Joyce et al., 2000; Seidov et al., 2019; Wu and He, 2024). However, there is a fundamental concern with using a fixed isotherm for diagnosing the GS path in a warming ocean: while the GS is likely to always be characterized by a strong north-south temperature gradient, it may not be the 15 ºC or 12 ºC isotherms, especially when background temperatures are rising (Garcia-Suarez and Fennel, 2024). Here we hypothesize that the T15 and T12 criteria overestimate a potential northward shift of the GS in a warming climate. Several previous studies have described limitations of temperature-based proxies for diagnosing the GS location. For example, air-sea heat fluxes can distort temperature gradients (Chen and Tung, 2018), and mesoscale eddies may bias the proxy northward (Chi et al., 2019). To the best of our knowledge, our hypothesis that background warming renders the temperature-based criteria unreliable has not be posed or systematically analyzed by others.

Because of the GS' meandering nature, it is challenging to analyze changes in its mean path. Wavelike fluctuations and eddies breaking off with faster currents than the GS itself make direct velocity observations ineffective for tracking the path east of 70°W (Fuglister and Voorhis, 1965). As a result, proxies like the above-mentioned T15 and T12 criteria are often used. Other commonly used proxies are based on sea surface height (SSH) from satellite altimetry (Andres, 2016; Chi et al., 2019; Rossby et al., 2014). The SSH-based proxies build on the concept that large-scale surface circulation follows SSH contours with the strongest currents flowing along the most tightly packed SSH contours. Although SSH data are available since 1993, these methods may not yet offer a long enough record to fully capture trends in the position of the GS (Chi et al., 2021). Chi et al. (2021) estimate that an additional 22–23 years of SSH observations are required to detect statistically significant trends. Todd and Ren (2023) used a dense observational data set consisting of Argo float measurements (since 2001) and underwater glider measurements (since 2015) to reconstruct the three-dimensional water properties of the Gulf Stream. They decomposed temperature and salinity signals as they contribute to changes in density, isolated the warming trend from a shift in the GS axis, and documented a modest northward shift of 6 ± 3 km per decade during their analysis period. Their method will become increasing useful as the record of autonomous observations grows.

The goals of this study are to 1) assess the reliability of the widely used temperature- and SSH-based proxies for tracking the position of the GS while the ocean is warming, and 2) test the hypothesis that the T15 proxy of the GS North Wall is inaccurate and overestimates a possible northward shift in a warming world. To this end, we analyze long-term preindustrial control and warming simulations from two widely used, high-resolution climate models, the CM2.6 model described in Delworth et al.

(2012) and used in Saba et al. (2016), Ceasar et al. (2021) and Claret et al. (2018) and the FOCI model described in Matthes et al. (2020) and subsequently used in Martin and Biastoch (2022), Martin et al. (2023) and Huo et al. (2024). We analyze a control and a warming simulation for each of the two climate models to explore the performance of different proxies over multiple decades into the future. Since the climate models are based on well-established dynamical principles, we believe they can be used to make inferences about the real ocean.

Our main finding is that the North Wall T15 criterion suggests a strong northward shift of the GS in the two widely used climate models that is not representative of the actual GS trajectory in those models. Since both models simulate pronounced shelf and slope warming, the results imply that such warming is not necessarily causally related to a northward GS shift. We thus caution against using temperature-based criteria in diagnosing changes in the GS path in warming scenarios.

2 Results

The FOCI and CM2.6 climate models (see Appendix A) show a pronounced warming trend along the continental slope and over the adjacent shelf in response to increasing atmospheric CO_2 in their warming simulations (Fig. 1). Both models reasonably simulate the key features of the northwest North Atlantic circulation, including the GS and Labrador Current (Fig. 2). These circulation patterns are consistent with previous studies demonstrating the skill of both models in simulating Gulf Stream dynamics and mesoscale variability, including studies that focussed on shifts in GS position using CM2.6 (Saba et al., 2016; Caesar et al., 2021) and applications of FOCI to mesoscale and frontal dynamics in the region (Matthes et al., 2020; Martin and Biastoch, 2022; Martin et al., 2023; Huo et al., 2024). The models also capture regional currents such as the shelfbreak jet and Nova Scotia current in both the control and warming runs (Fig. 2 b-d). These currents, however, are not resolved in satellite SSH observations due to the insufficient horizontal resolution (0.25°; Fig. 2a). In CM2.6, the GS velocity axis becomes diffuse near and beyond the New England Seamounts (Fig. 2 d, e). Still, both models reproduce GS paths similar to those observed in satellite data (Fig. 2).

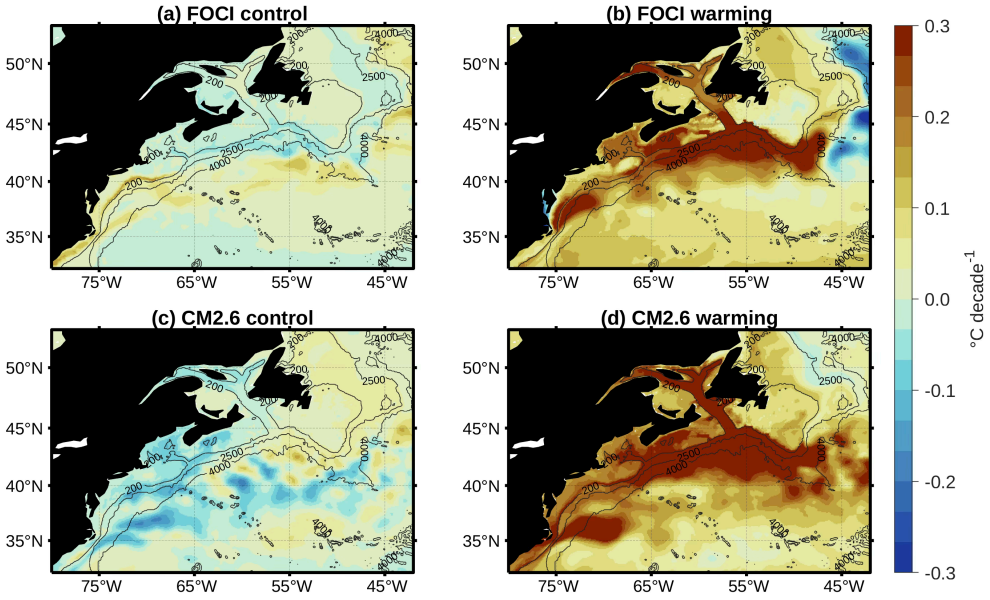

Figure 1 Linear trends in annual-mean bottom (or 200 m where the water column is deeper than 200 m) temperature between 2015 and 2100 for (a) FOCI control, (b) FOCI warming, (c) CM2.6 control, and (d) CM2.6 warming simulations. Trends are calculated from annual means.

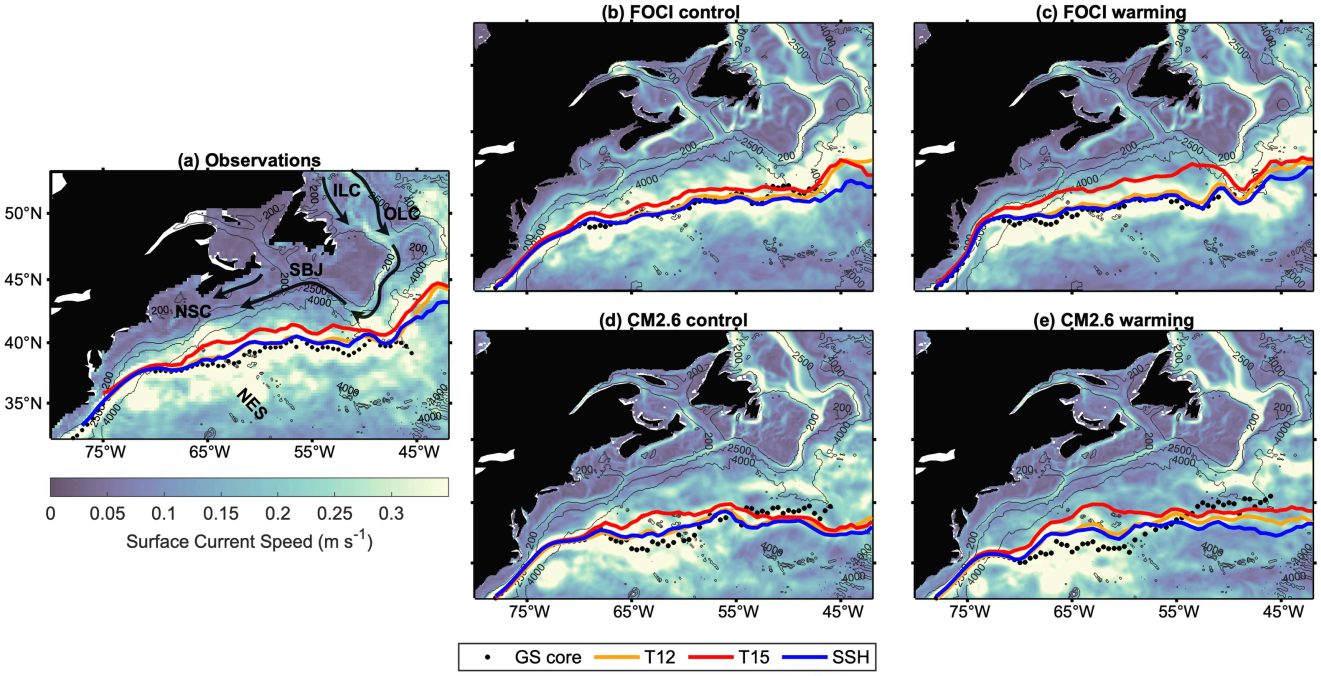

Figure 2 Annual mean surface velocity and GS position from observations (a), FOCI (b, c), and CM2.6 (d, e) in 2015. Background shading shows the mean surface current speed (m s^{-1}). Orange contours are the 12 °C isotherm at 450 m depth (T12). Red contours indicate the 15 °C isotherm at 200 m depth (T15). Blue contours show the SSH of -0.23 m for CM2.6, 0.1 m for FOCI, and 0.25 m for the observations. Black points represent the locations of maximum surface velocity (GS core). Black arrows in a) show the approximate location of the Nova Scotia current (NSC), shelfbreak jet (SBJ) and the inner (ICL) and outer (OLC) Labrador Current. NES: New England Seamounts.

We tested T15, T12, and four SSH-based criteria for diagnosing the true GS path, defined as the maximum velocity or GS core (see Appendix A). Among the SSH methods, the maximum SSH variance criterion performs poorly when applied to monthly averaged fields (Fig S1) and the skewness criterion underperforms in the CM2.6 control scenario, likely due to sensitivity to small-scale turbulence and eddies (Fig. S2). Despite its high resolution, CM2.6 does not appear to capture the sharp gradients needed for accurate skewness detection (Fig. S3). The other two SSH-based criteria appear more robust, with the criterion based on the location of a specific SSH isoline being closest to the axis of maximum velocity in both simulations (Fig. S4). Thus, criteria based on skewness, variance, and maximum gradient will not be used further in this study.

First, we consider the performance of the T15, T12 and SSH-based criteria in the year 2015 (Fig. 2, 3). Close to Cape Hatteras (west of 74° W), the GS is attached to the shelf break, and all criteria follow the axis of maximum surface velocity in both models and satellite observations (Fig. 2) to within 0.3º of latitude (33 km; Fig. 3). In observations, once the GS detaches from the shelf at ~74° W, T15 stays close to the maximum velocity axis until reaching 67° W. Downstream (east) of this longitude, T15 diverges and is located to the north of the GS core by ~1.4° (150 km; Fig. 2a), while the T12 and the SSH-based proxies track the GS core more closely (within 0.7° for T12 and 0.5° for SSH). The model simulations allow us to distinguish between preindustrial and warming scenarios. In the preindustrial simulations of both models, T15 is located northward of the GS core (by up to 1° in FOCI and 1.3° in CM2.6) while T12 and SSH are most faithful to the core of the GS in FOCI (within 0.2°) and biased northward by up to 0.5° in CM2.6 (dotted lines in Fig. 3, c). In the warming simulations in 2015, both temperature proxies (T15 and T12) are markedly biased northward with T15 exceeding distances from the GS core of 2° in FOCI and up to 2.3°, or ~250 km, in CM2.6 (solid lines in Fig 3.b, c) while the SSH proxy is equally close to the GS core in both pre-industrial and warming simulations. When comparing the northward bias of the two temperature criteria between preindustrial and warming simulations it appears that the northward bias roughly doubles in both models because of ocean warming. In summary, already in 2015 it appears that the T15 criterion is biased northward in observations and in the two warming simulations. A qualitatively similar bias applies to the T12 criterion although it is smaller in magnitude. The SSH criterion follows the GS core more faithfully.

Next, we consider the performance of these criteria in the warming scenarios up to 2100. Figure 4 shows the annual mean location of the GS path diagnosed by the T12, T15 and SSH criteria for the years 2015 to 2100. In FOCI it appears that the T12 criterion remains in place latitudinally, with some interannual fluctuations, while the T15 criterion moves northward, ultimately attaching to the shelf break along the Scotian Shelf and the Grand Banks, and the SSH criterion moves southward. In CM2.6, all criteria appear to suggest a northward movement that is most pronounced for T15 and smallest for the SSH.

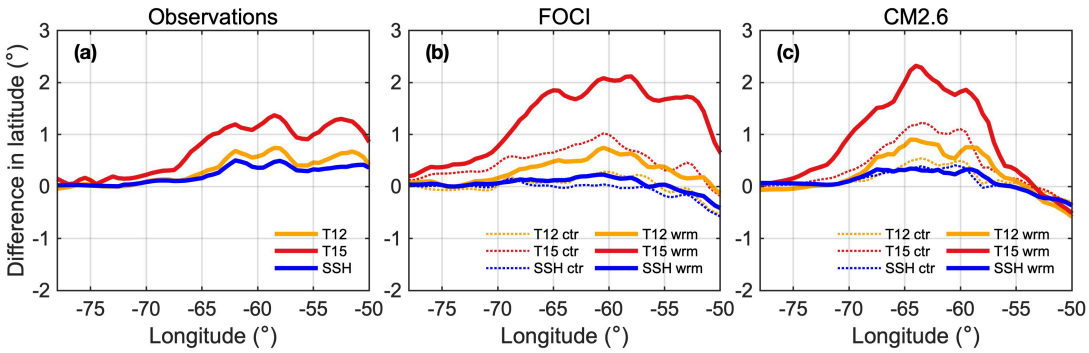

Figure 3 Differences between the GS position estimated by different criteria and the latitude of maximum velocity across different longitudes under control (ctr; dotted lines) and warming scenarios (wrm; solid lines) for observational data (a) and the FOCI (b) and CM2.6 (c) climate models in 2015. The orange (T12) and red (T15) lines correspond to the two temperature-based criteria, and the blue (SSH) lines indicate the SSH-based criterion.

A more quantitative assessment is presented in Figure 5, where the evolution of the mean latitude of the GS core is presented for sections A1 (75° to 70° W) and A2 (71° to 50° W) from 2015 to 2100 (black line) as well as its diagnosed location using the T12, T15 and SSH criteria (orange, red and blue lines). Close to Cape Hatteras (section A1) the GS moves north slightly in FOCI and more pronounced in CM2.6. The T12 and SSH criteria track its location closely in both models. However, already in 2015, the T15 criterion is biased northward in both models, and the size of the bias grows until 2100. In both models, the rate of the northward movement of T15 is more than twice that of the GS core. In section A2 (east of 71° W) the GS core moves southward slightly in FOCI (by 0.02° per decade). This southward move is captured qualitatively by the SSH criterion (which moves southward by 0.06° per decade) but not by the T12 and T15 criteria which move northward by 0.02° per decade and 0.13° per decade, respectively. In CM2.6, the GS core moves northward by 0.08° per decade. This movement is represented well by the SSH criterion which moves northward by 0.11° per decade. The latitude of the GS core is overestimated by the T12 and T15 criteria already in 2015 and the size of the bias grows until 2100. T15 suggests a northward migration of the GS of 0.2° per decade which is more than twice the actual northward migration of the core in CM2.6 of 0.08° per decade. In summary, in the warming simulations neither of the temperature criteria accurately represents the location of the GS core east of 71° W and both significantly overestimate its possible northward movement. Notably, both temperature criteria suggest a northward movement in FOCI east of 71° W even though the GS core moves southward in this simulation.

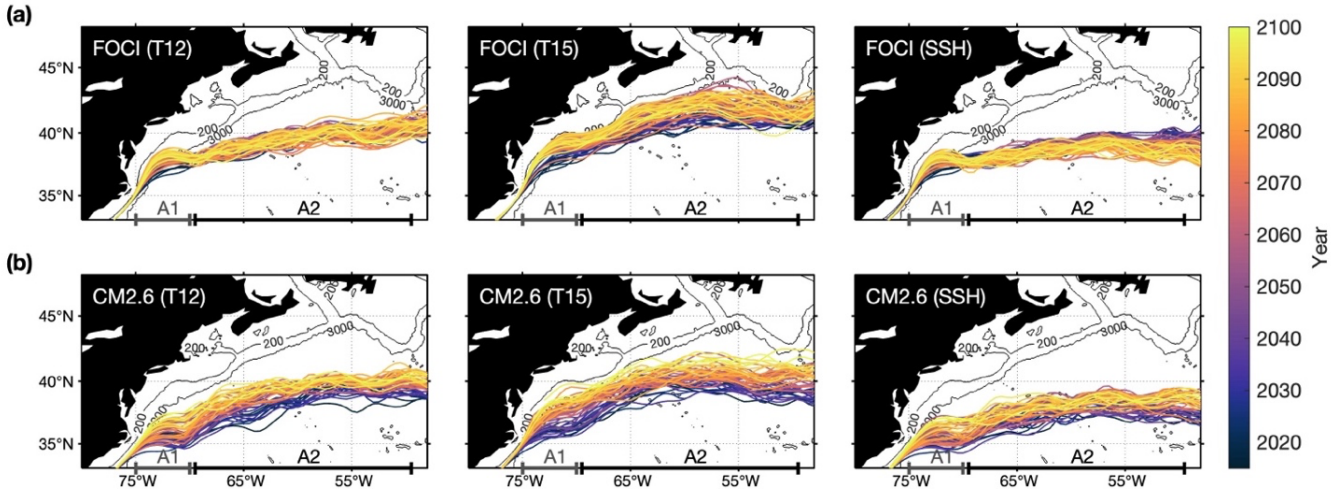

Figure 4 Annual mean location of the GS path based on temperature (T12 and T15) and SSH criteria in the warming simulations of FOCI (a) and CM2.6 (b). Colors indicate different years from 2015 to 2100. Regions A1 and A2 (shown along the x-axis) indicate the longitude bands over which latitudes are averaged in Figure 5.

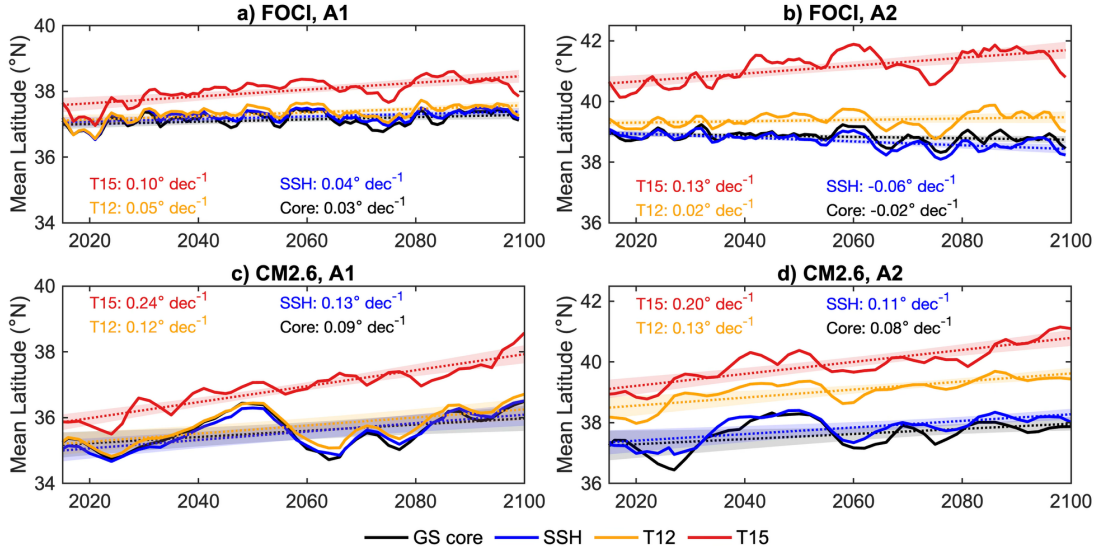

Figure 5 Mean latitude of the temperature-based (T12 and T15) and SSH-based Gulf Stream path criteria averaged over two regions: A1 (75° W to 70° W, grey bracket in Fig. 4) and A2 (71° W to 50° W, black bracket in Fig. 4) in FOCI (a, b) and CM2.6 (c, d) simulations. Solid lines show the annual mean latitude of each proxy, along with the reference Gulf Stream core position (GS core). Dotted lines indicate the corresponding linear trends, and shaded bands represent the 95% confidence interval of the fitted mean trend. Trend magnitudes (in ° latitude per decade) are reported within each panel for each proxy. Trend statistics are provided in Table S1.

The growing discrepancy between temperature-based trajectories and the actual GS path in the warming scenarios is due to progressive warming of the slope region. In Figure 6, we show the evolution of annual average temperature from 2025 to 2100 for the slope and subtropical regions at the surface and at 200 and 450 m depth for both the control (dotted lines) and warming (solid lines) simulations. Both models project warming in the slope and subtropical regions that exceed natural variability at all depths shown (Fig. 6). Warming in the slope region occurs at twice the rate of the subtropical region, with linear trends

ranging from 0.12 °C to 0.29 °C per decade in the slope region, compared to 0.06 °C to 0.11 °C per decade in the subtropical region (Table S2). Within the slope region, the temperature rise is more pronounced at 200 m depth than at the surface and at 450 m in both models. FOCI projects a rise of 0.12 °C, 0.22ºC, and 0.17 ºC per decade at the surface, 200 m, and 450 m depths, respectively. In CM2.6, the warming trends are 0.25 °C, 0.29 °C, and 0.18 ºC per decade at the surface, 200 m, and 450 depth, respectively. The warming of the slope region results in an apparent northward shift of the GS path when inferred from a fixed isotherm as is done with both temperature-based criteria (especially with T15 at 200 m; to a lesser extent with T12 at 450 m depth), but the magnitude of this shift (and its direction in the case of A2 in FOCI) does not reflect actual shifts in latitude of the GS core.

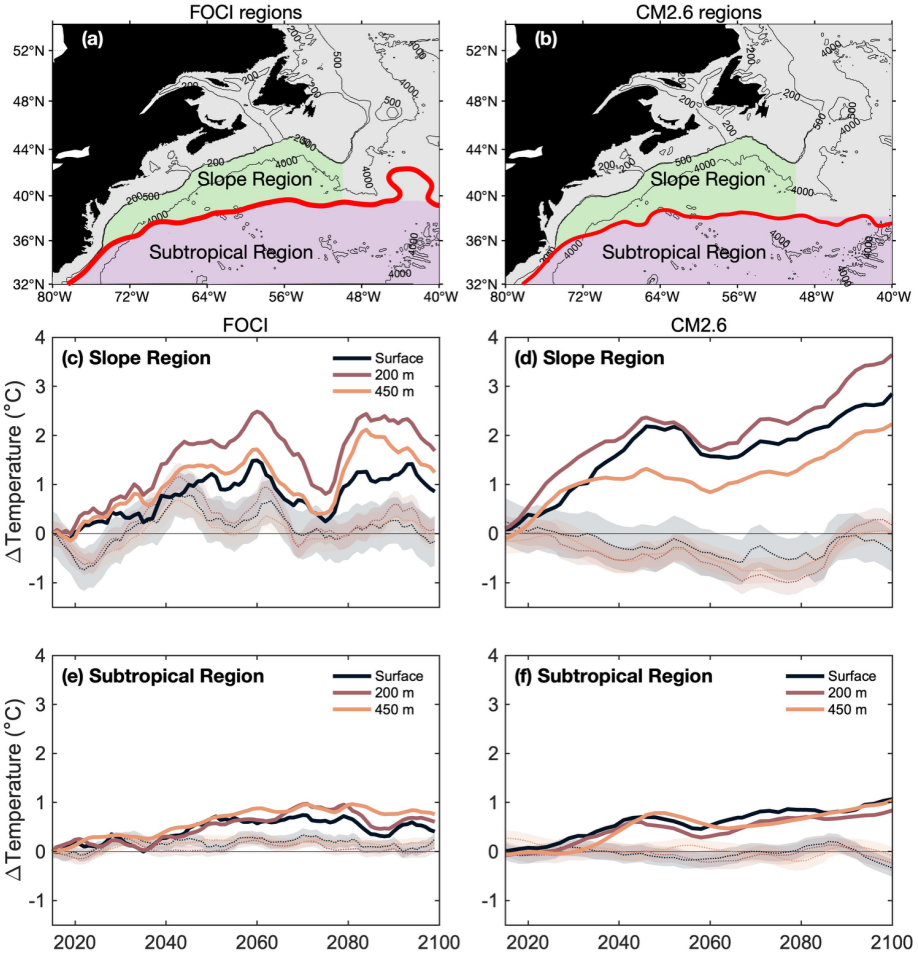

Figure 6 Changes in seawater temperature in the slope and subtropical regions of the northwest North Atlantic from the FOCI and CM2.6 models. The top panels (a, b) show the defined regions: the slope region (green) and the subtropical region (purple) with the red contour marking the mean Gulf Stream path from the control simulation. The middle (c, d) and bottom (e, f) panels depict the temperature change (ΔTemperature) relative to the 2015 annual mean. Solid lines correspond to the warming runs, and dotted lines to the control runs, with shaded areas showing one standard deviation around the annual mean (natural variability). The left column (a, c, e) shows results from the FOCI model, and the right column (b, d, f) shows results from the CM2.6 model. Trend statistics are provided in Table S2.

3 Discussion

Our main goal in this study was to assess whether temperature- and SSH-based criteria for diagnosing the path of the GS are reliable in a warming ocean. To address this, we analyzed preindustrial control and warming simulations from two high-resolution climate models, FOCI and CM2.6. Both models project a rapid warming of bottom waters on the northwest North Atlantic shelves (0.14- 0.46°C per decade) and in the slope region of 0.12-0.38 °C per decade in the upper 200 m, a rate that is two to three times faster than in the adjacent subtropical region. These projections are consistent with in situ observations reporting similar warming in the slope waters (Gonçalves Neto et al., 2021; Seidov et al., 2019; Todd and Ren, 2023).

In both models, the temperature-based criteria (T12 and T15) suggest pronounced northward shifts in the GS path in the warming scenarios that do not match the actual shifts of the GS core and do not occur in the pre-industrial simulations. In the pre-industrial control runs of both models, the SSH and T12 criteria closely predict the location of the GS core while T15 is biased northward (see Fig. 3b, c). In the warming simulations already in 2015, the T12 and T15 are located well northward of their pre-industrial analogs, while the SSH criterion remains closely aligned with the GS core (Fig. 3b, c). The same appears to be the case for observations (Fig 3a), at least qualitatively, although we cannot separate the warming contribution from the pre-industrial, because observations for the latter are not available. The evolution of the mean latitude of the GS from 2025 to 2100 differs between FOCI and CM2.6. In FOCI, the GS core east of 71° W moves slightly southward by 0.02° per decade while T12 and T15 move northward by 0.02° per decade and 0.13° per decade, respectively (Fig. 5). In CM2.6, the GS core east of 71° W moves northward by northward by 0.08° per decade while T12 and T15, both already located significantly further north than the GS core in 2015, move northward by 0.13° per decade and 0.20° per decade, respectively (Fig. 5). In other words, while the North Wall closely follows the axis of maximum velocity near Cape Hatteras (west of 74 °W), east of 71° W the GS location diagnosed by T15 is located significantly to the north of the GS core and moves further northward until 2100 at a much faster rate than the GS core (at more than twice the rate in the case of CM2.6; in the opposite direction in FOCI). The SSH criterion follows the location of the GS core well in all cases and thus appears to be a reliable proxy for diagnosing the GS location under warming conditions.

The climatological location of the North Wall has previously been reported to poorly match the GS high-velocity core. Chi et al. (2019) showed that the T15-based North Wall frequently lies north of the velocity maximum due to mesoscale eddy activity and frontal meandering. Frankignoul et al. (2001) demonstrated that the thermal front responds strongly to atmospheric forcing and does not consistently coincide with the dynamical jet. Pérez-Hernández and Joyce (2014) similarly found a poor agreement between a temperature-based index derived from T15 and altimeter-based Gulf Stream path indices between 2000 and 2011. These studies highlight present-day limitations of temperature-based indices. Our work goes further by showing that, in a warming ocean, background temperature increases systematically push T15 and T12 northward even when the GS core does

not move, amplifying their bias under anthropogenic warming and making temperature-based criteria fundamentally inadequate for tracking the full extent of the GS path in such cases.

Our finding that the T15 criterion cannot reliably diagnose a northward shift of the GS is significant because a widely accepted hypothesis links the rapid ocean warming observed in the northwest North Atlantic to a northward migration of the GS (Caesar et al., 2018; Gonçalves Neto et al., 2021; Saba et al., 2016; Todd and Ren, 2023). This conclusion is largely based on the apparent shift of the North Wall, defined by the 15°C isotherm at 200 m depth, i.e. the T15 criterion (Caesar et al., 2018; Seidov et al., 2019; Wu and He, 2024). These findings align with results from Alexander et al. (2020), who showed that enhanced warming on the northwest Atlantic shelf, particularly in the Gulf of Maine and Gulf of St. Lawrence, can result from multiple processes not necessarily linked to a northward migration of the Gulf Stream. These include local atmospheric warming, increased heat uptake, and the advection of warmer Arctic and Labrador Sea waters by the Labrador Current, as well as mesoscale eddy activity in the Gulf Stream region. Such mechanisms offer plausible alternatives for explaining regional warming trends without invoking large-scale latitudinal shifts in the GS.

Our analysis indicates that rising upper-slope temperatures bias the temperature-based estimates, making the North Wall an unreliable indicator of long-term circulation changes. While temperature signals are widely used in paleoclimate reconstructions due to their apparent links to ocean dynamics (Caesar et al., 2021; Palter, 2015), our findings suggest that care is needed when inferring past or future changes in northwest Atlantic circulation solely from temperature-based methods. Reconstruction of surface or subsurface temperature patterns in the Atlantic Ocean is a common approach to constraining the strength of the AMOC (Caesar et al., 2021; Rahmstorf et al., 2015; Thornalley et al., 2018). However, our results indicate that temperature patterns alone may provide a limited or biased representation of ocean currents dynamics. We caution against using the North Wall to infer future or present changes in the GS trajectory. Instead, we recommend using an SSH-based criterion.

4 Conclusions

The T15 and T12 criteria for the GS North Wall, both temperature-based proxies for the GS location, overestimate the northward shift of the GS in a warming ocean and thus create the misleading appearance of the GS rapidly migrating north. In contrast, the SSH-based criterion remains more closely aligned with the GS core, making it a more reliable tool for path estimations. The discrepancies between the temperature-based proxies and true GS core location arise because the slope region is rapidly warming. Our results call into question the notion that warming in the northwest North Atlantic is causally related to a northward migration of the GS. Future research should focus on elucidating alternative hypotheses for the observed warming in the slope region and on determining the underlying drivers.

Appendices A: Methods

A.1 Models and observations

A.1.1 Climate model simulations

Monthly outputs from the climate model CM2.6 and the Flexible Ocean Climate Infrastructure (FOCI) model are used to investigate the long-term changes in the location of the GS under both preindustrial and high CO_2 emission scenarios. These models are particularly suited for examining changes in ocean circulation due to their high-resolution capabilities and ability to simulate mesoscale processes (Matthes et al., 2020; Saba et al., 2016).

The CM2.6, developed by the Geophysical Fluid Dynamics Laboratory (GFDL), includes an atmospheric general circulation model at an average spatial resolution of 0.5° (50 km) and an ocean component with resolution of 0.1° (10 km) and 50 vertical layers. After a 120-year spin-up phase at preindustrial CO_2 levels (286 ppm), two simulations were performed for 80 additional years: a preindustrial control run with constant CO_2 at 286 ppm (control run), and a transient run where CO_2 increased by 1% per year for 70 years until it doubled and then remained at this level for 10 additional years (warming run). Further details of the model and simulations can be found in Delworth et al. (2012). The time dimension of the warming run aligns with the Representative Concentration Pathway 6 (RCP6) scenario, as described by Claret et al. (2018) and Garcia-Suarez and Fennel (2024).

The FOCI is an Earth system model developed at the GEOMAR Helmholtz Centre for Ocean Research Kiel built on the NEMO v3.6. model (Madec, 2016) and coupled to the ECHAM6.3 atmosphere (Müller et al., 2018), JSBACH land (Reick et al., 2013), and LIM2 sea-ice (Fichefet and Maqueda, 1997) models using the coupler OASIS3-MCT (Valcke, 2013). The physical ocean model components in FOCI are detailed in Matthes et al. (2020). Atmosphere and land components are applied to a T63 (1.9°) grid with the atmosphere having 95 vertical levels. The ocean grid covers the entire globe with a ORCA05 grid (0.5° horizontal resolution) with 46 vertical levels. FOCI is capable of applying a two-way high-resolution regional ocean nesting through the adaptive grid refinement AGRIF (Debreu et al., 2008). In this study we used the VIKING10 nest, as introduced by Matthes et al. (2020), which enhances the horizontal resolution in the North Atlantic Ocean by a factor 5 (from 0.5° to 0.1°) and enables resolution of mesoscale ocean fronts and eddies. The VIKING10 nested configuration was used to perform two simulations: a preindustrial control run (control run) and a simulation based on the SSP5-3.4-os scenario (O'Neill et al., 2016). The latter, hereafter called warming run, follows an overshoot pathway, where atmospheric CO_2 emissions increase significantly until 2040, followed by an aggressive mitigation to reduce emissions to zero by approximately 2070, with substantial negative global emissions (i.e., CO_2 removal) afterward until 2100. Details of both simulations can be found in Keller et al. (2023).

Both model configurations have been extensively evaluated and applied in studies of North Atlantic circulation and mesoscale dynamics. The same CM2.6 simulation used here has supported numerous investigations into GS variability, including analyses of lateral shifts (Caesar et al., 2021; Saba et al., 2016) and biogeochemical responses (Claret et al., 2018). Likewise, although more recently developed, the FOCI configuration has been validated in detail (Matthes et al., 2020) and is now

routinely employed to investigate mesoscale processes in the North Atlantic (Huo et al., 2024; Martin et al., 2022; Martin and Biastoch, 2023).

A.1.2 Satellite altimetry

Altimetric data used to determine the position of the GS is derived from the daily 0.25° delayed time merged absolute dynamic topography, hereafter referred to as sea surface height (SSH), and the corresponding surface geostrophic velocity provided by the Copernicus Marine and Environment Monitoring Service (http://www.marine.copernicus.eu). Daily maps are averaged to produce monthly maps spanning 2015 to 2023.

A.1.3 Armor3D

Sea surface temperature (SST) and temperature at 200 m depth are extracted from Armor3D (v4), a 0.25°-gridded, 3D observation-based reanalysis product. This dataset reconstructs seawater temperature by integrating satellite-derived measurements with in situ observations, as described by Guinehut et al. (2012) and Mulet et al. (2012). Chi et al. (2018) assessed the accuracy of Armor3D in the GS region, concluding that its temperature fields resolve the longitudinal structure of the GS better than coarser temperature products. Monthly means of Armor3D data used in this study are provided by the Copernicus Marine and Environment Monitoring Service (http://www.marine.copernicus.eu).

A.2 Criteria of the GS path

We define the true axis of the GS as the location of the local surface current speed maximum, estimated as the highest velocity along meridional lines spaced 0.1° apart for model output and 0.25° apart for observational data, between 78°W and 50°W. In cases where the GS crosses the same longitude multiple times due to the presence of eddies and meanders, we selected the maximum velocity closest in longitude to the previous estimate. Using this axis of maximum velocity as a reference, we evaluated the performance of four criteria for estimating the GS position: two temperature-based criteria and four SSH-based criteria. These criteria were assessed under present-day, preindustrial, and rapid warming scenarios.

A.2.1 Temperature-based criteria

The first temperate-based criterion evaluated is the North Wall, a sharp temperature front that delineates the GS from the slope water, commonly represented by the 15°C isotherm (T15) at 200 m depth (Cornillon and Watts, 1987; Fuglister and Voorhis, 1965). Several studies using observational or modeled datasets have assumed the location of this isotherm to coincide with the GS path (Caesar et al., 2018; Claret et al., 2018; Peterson et al., 2017; Seidov et al., 2019). The second criterion is the location of the 12°C isotherm (T12) at 450 m depth, as proposed by Sánchez-Román et al. (2024), which is believed to more accurately follow the trajectory of the GS and limit the influence of short-term surface variations of seawater temperature.

A.2.3 SSH-based criteria

Large-scale surface circulation generally follows SSH contours (Häkkinen, 2001). The 0.25-m SSH contour is often used as a proxy for the GS path in altimetry data due to its proximity to the maximum velocity axis (Andres, 2016; Chi et al., 2019; Lillibridge and Mariano, 2013). In this manuscript, we therefore use the 0.25-m SSH contour as a proxy when analyzing altimetry data. However, it is important to note that the specific SSH contour associated with the GS in a numerical model may differ from that in observations as SSH in models typically refers to a different geoid than altimetry data. Here, we evaluated different SSH contours and selected the -0.23 m contour for CM2.6 and 0.1 m for FOCI, as these contours showed the shortest mean distance to the points of maximum surface velocity in the corresponding models in the control runs. Small changes in this value do not affect any of the conclusions of this study. The second SSH-based criterion corresponds to the sea level zero-skewness contour calculated annually from monthly fields of observed and simulated SSH from 2015 to 2023 (Fig. S2). Zero skewness has been shown to represent the path of the GS in its free jet segment (Thompson and Demirov, 2006). The other two SSH-based criteria considered are: the location of the maximum SSH gradient along meridional lines (Lillibridge and Mariano, 2013; Peña-Molino and Joyce, 2008); and the latitude where the variance of the monthly mean SSH anomaly is highest. Here, the SSH anomaly is defined as the difference between the monthly mean SSH and a 6-year calendar month mean). This criterion is adapted from Pérez-Hernández and Joyce (2014), following Ross et al. (2023).

All criteria described above are derived from monthly averaged fields. For each year, the 12 monthly mean paths are divided into 0.5° longitude bins and averaged to produce the multiyear means analyzed below. Finally, to quantify the migration of the GS, we averaged the latitude of each criterion across two longitude ranges: A1 (75ºW to 70ºW) and A2 (71ºW to 50ºW). This averaging approach is preferred in this study over the widely used method of analyzing the time series at fixed locations (Gangopadhyay et al., 2016; Joyce et al., 2000; Taylor and Stephens, 1998), as the latter may introduce errors by incorporating increased meander frequency or amplitude, which could be misinterpreted as GS lateral movement or slowing.

Data Availability

The all-satellite merged 0.25° SSH (DUACS delayed-time altimeter gridded data) and ARMOR3D (v4) products are freely available from the Copernicus Climate Change Service (2021) and the European Union-Copernicus Marine Service (2020), respectively. The processed data from the CM2.6 and FOCI climate models used in this study are available on Zenodo via Garcia-Suarez et al. (2025).

Supplement

The supplement related to this article will be available online at the DOI link upon acceptance.

Author Contribution

LGS and KF defined the overall research problem and methodology. LGS carried out the analysis and led the writing of the manuscript in close collaboration with KF. NM, TK, and DPK performed FOCI simulations. All coauthors reviewed and edited the manuscript.

Competing interests

The authors declare that they have no conflict of interest

Acknowledgments

We thank Jasmin John for making CM2.6 model output available to us. We acknowledge financial support from NSERC through the COD-REMAP project and KF's Discovery Grant and from the Ocean Frontier Institute through the NWA-BCP project. LGS gratefully acknowledges support from the Nova Scotia Graduate Scholarship program. We also acknowledge computational resources provided by the Digital Research Alliance of Canada.

References

Alexander, M. A., Shin, S., Scott, J. D., Curchitser, E., and Stock, C.: The Response of the Northwest Atlantic Ocean to Climate Change, Journal of Climate, 33, 405–428, https://doi.org/10.1175/JCLI-D-19-0117.1, 2020.

Andres, M.: On the recent destabilization of the Gulf Stream path downstream of Cape Hatteras, Geophys. Res. Lett., 43, 9836–9842, https://doi.org/10.1002/2016GL069966, 2016.

Bisagni, J. J., Gangopadhyay, A., and Sanchez-Franks, A.: Secular change and inter-annual variability of the Gulf Stream position, 1993–2013, 70°−55°W, Deep Sea Research Part I: Oceanographic Research Papers, 125, 1–10, https://doi.org/10.1016/j.dsr.2017.04.001, 2017.

Caesar, L., Rahmstorf, S., Robinson, A., Feulner, G., and Saba, V.: Observed fingerprint of a weakening Atlantic Ocean overturning circulation, Nature, 556, 191–196, https://doi.org/10.1038/s41586-018-0006-5, 2018.

Caesar, L., McCarthy, G. D., Thornalley, D. J. R., Cahill, N., and Rahmstorf, S.: Current Atlantic Meridional Overturning Circulation weakest in last millennium, Nat. Geosci., 14, 118–120, https://doi.org/10.1038/s41561-021-00699-z, 2021.

Chen, X. and Tung, K.-K.: Global surface warming enhanced by weak Atlantic overturning circulation, Nature, 559, 387–391, https://doi.org/10.1038/s41586-018-0320-y, 2018.

Chi, L., Wolfe, C. L. P., and Hameed, S.: Intercomparison of the Gulf Stream in ocean reanalyses: 1993−2010, Ocean Modelling, 125, 1–21, https://doi.org/10.1016/j.ocemod.2018.02.008, 2018.

Chi, L., Wolfe, C. L. P., and Hameed, S.: The Distinction Between the Gulf Stream and Its North Wall, Geophys. Res. Lett., 46, 8943–8951, https://doi.org/10.1029/2019GL083775, 2019.

Chi, L., Wolfe, C. L. P., and Hameed, S.: Has the Gulf Stream Slowed or Shifted in the Altimetry Era?, Geophysical Research Letters, 48, e2021GL093113, https://doi.org/10.1029/2021GL093113, 2021.

Claret, M., Galbraith, E. D., Palter, J. B., Bianchi, D., Fennel, K., Gilbert, D., and Dunne, J. P.: Rapid coastal deoxygenation due to ocean circulation shift in the northwest Atlantic, Nature Clim Change, 8, 868–872, https://doi.org/10.1038/s41558-018-0263-1, 2018.

Copernicus Climate Change Service: GLOBAL OCEAN GRIDDED L4 SEA SURFACE HEIGHTS AND DERIVED VARIABLES REPROCESSED (COPERNICUS CLIMATE CHANGE SERVICE), https://doi.org/10.48670/MOI-00145, 2021.

Cornillon, P. and Watts, R.: Satellite Thermal Infrared and Inverted Echo Sounder Determinations of the Gulf Stream Northern Edge, Journal of Atmospheric and Oceanic Technology, 4, 712–723, https://doi.org/10.1175/1520-0426(1987)004%253C0712:STIAIE%253E2.0.CO;2, 1987.

Debreu, L., Vouland, C., and Blayo, E.: AGRIF: Adaptive grid refinement in Fortran, Computers & Geosciences, 34, 8–13, https://doi.org/10.1016/j.cageo.2007.01.009, 2008.

Delworth, T. L., Rosati, A., Anderson, W., Adcroft, A. J., Balaji, V., Benson, R., Dixon, K., Griffies, S. M., Lee, H.-C., Pacanowski, R. C., Vecchi, G. A., Wittenberg, A. T., Zeng, F., and Zhang, R.: Simulated Climate and Climate Change in the GFDL CM2.5 High-Resolution Coupled Climate Model, Journal of Climate, 25, 2755–2781, https://doi.org/10.1175/JCLI-D-11-00316.1, 2012.

European Union-Copernicus Marine Service: Multi Observation Global Ocean 3D Temperature Salinity Height Geostrophic Current and MLD, https://doi.org/10.48670/MOI-00052, 2020.

Fichefet, T. and Maqueda, M. A. M.: Sensitivity of a global sea ice model to the treatment of ice thermodynamics and dynamics, Journal of Geophysical Research: Oceans, 102, 12609–12646, https://doi.org/10.1029/97JC00480, 1997.

Forsyth, J. S. T., Andres, M., and Gawarkiewicz, G. G.: Recent accelerated warming of the continental shelf off New Jersey: Observations from the CMV Oleander expendable bathythermograph line, Journal of Geophysical Research: Oceans, 120, 2370–2384, https://doi.org/10.1002/2014JC010516, 2015.

Frankignoul, C., de Coëtlogon, G., Joyce, T. M., and Dong, S.: Gulf Stream Variability and Ocean–Atmosphere Interactions, J. Phys. Oceanogr., 31, 3516–3529, https://doi.org/10.1175/1520-0485(2002)031%253C3516:GSVAOA%253E2.0.CO;2, 2001.

Fuglister, F. C. and Voorhis, A. D.: A New Method of Tracking the Gulf Stream1, Limnology and Oceanography, 10, R115–R124, https://doi.org/10.4319/lo.1965.10.suppl2.r115, 1965.

Gangopadhyay, A., Chaudhuri, A. H., and Taylor, A. H.: On the Nature of Temporal Variability of the Gulf Stream Path from 75° to 55°W, Earth Interactions, 20, 1–17, https://doi.org/10.1175/EI-D-15-0025.1, 2016.

Garcia-Suarez, L. and Fennel, K.: Physical Drivers and Biogeochemical Effects of the Projected Decline of the Shelfbreak Jet in the Northwest North Atlantic Ocean, Journal of Advances in Modeling Earth Systems, 16, e2024MS004580, https://doi.org/10.1029/2024MS004580, 2024.

Gonçalves Neto, A., Langan, J. A., and Palter, J. B.: Changes in the Gulf Stream preceded rapid warming of the Northwest Atlantic Shelf, Commun Earth Environ, 2, 74, https://doi.org/10.1038/s43247-021-00143-5, 2021.

Guinehut, S., Dhomps, A.-L., Larnicol, G., and Le Traon, P.-Y.: High resolution 3-D temperature and salinity fields derived from in situ and satellite observations, Ocean Science, 8, 845–857, 2012.

Häkkinen, S.: Variability in sea surface height: A qualitative measure for the meridional overturning in the North Atlantic, Journal of Geophysical Research: Oceans, 106, 13837–13848, https://doi.org/10.1029/1999JC000155, 2001.

Hansen, D. V.: Gulf stream meanders between Cape Hatteras and the Grand Banks, Deep Sea Research and Oceanographic Abstracts, 17, 495–511, https://doi.org/10.1016/0011-7471(70)90064-1, 1970.

Huo, W., Drews, A., Martin, T., and Wahl, S.: Impacts of North Atlantic Model Biases on Natural Decadal Climate Variability, Journal of Geophysical Research: Atmospheres, 129, e2023JD039778, https://doi.org/10.1029/2023JD039778, 2024.

Johnson, G. C. and Lyman, J. M.: Warming trends increasingly dominate global ocean, Nat. Clim. Chang., 10, 757–761, https://doi.org/10.1038/s41558-020-0822-0, 2020.

Joyce, T. M., Deser, C., and Spall, M. A.: The Relation between Decadal Variability of Subtropical Mode Water and the North Atlantic Oscillation*, J. Climate, 13, 2550–2569, https://doi.org/10.1175/1520-0442(2000)013%253C2550:TRBDVO%253E2.0.CO;2, 2000.

Keller, D. P., Mehendale, N., and Kemena, T.: Analysis (report) of high- resolution modelling of efficacy, and regional impacts of selected ocean NETs close to the deployment sites, 2023.

Lillibridge, J. L. and Mariano, A. J.: A statistical analysis of Gulf Stream variability from 18+ years of altimetry data, Deep Sea Research Part II: Topical Studies in Oceanography, 85, 127–146, https://doi.org/10.1016/j.dsr2.2012.07.034, 2013.

Ma, X., Jia, Y., and Han, Z.: Impact of the Gulf Stream front on atmospheric rivers and Rossby wave train in the North Atlantic, Clim Dyn, https://doi.org/10.1007/s00382-024-07178-2, 2024.

Madec, G.: NEMO ocean engine. Note du Pôle de modélisation de l'Institut Pierre-Simon Laplace 27, 386 pp, 2016.

Martin, T. and Biastoch, A.: On the ocean's response to enhanced Greenland runoff in model experiments: relevance of mesoscale dynamics and atmospheric coupling, Ocean Science, 19, 141–167, https://doi.org/10.5194/os-19-141-2023, 2023.

Martin, T., Biastoch, A., Lohmann, G., Mikolajewicz, U., and Wang, X.: On Timescales and Reversibility of the Ocean's Response to Enhanced Greenland Ice Sheet Melting in Comprehensive Climate Models, Geophysical Research Letters, 49, e2021GL097114, https://doi.org/10.1029/2021GL097114, 2022.

Matthes, K., Biastoch, A., Wahl, S., Harlaß, J., Martin, T., Brücher, T., Drews, A., Ehlert, D., Getzlaff, K., Krüger, F., Rath, W., Scheinert, M., Schwarzkopf, F. U., Bayr, T., Schmidt, H., and Park, W.: The Flexible Ocean and Climate Infrastructure version 1 (FOCI1): mean state and variability, Geoscientific Model Development, 13, 2533–2568, https://doi.org/10.5194/gmd-13-2533-2020, 2020.

Mulet, S., Rio, M.-H., Mignot, A., Guinehut, S., and Morrow, R.: A new estimate of the global 3D geostrophic ocean circulation based on satellite data and in-situ measurements, Deep Sea Research Part II: Topical Studies in Oceanography, 77, 70–81, 2012.

Müller, W. A., Jungclaus, J. H., Mauritsen, T., Baehr, J., Bittner, M., Budich, R., Bunzel, F., Esch, M., Ghosh, R., Haak, H., Ilyina, T., Kleine, T., Kornblueh, L., Li, H., Modali, K., Notz, D., Pohlmann, H., Roeckner, E., Stemmler, I., Tian, F., and Marotzke, J.: A Higher-resolution Version of the Max Planck Institute Earth System Model (MPI-ESM1.2-HR), Journal of Advances in Modeling Earth Systems, 10, 1383–1413, https://doi.org/10.1029/2017MS001217, 2018.

O'Neill, B. C., Tebaldi, C., van Vuuren, D. P., Eyring, V., Friedlingstein, P., Hurtt, G., Knutti, R., Kriegler, E., Lamarque, J.-F., Lowe, J., Meehl, G. A., Moss, R., Riahi, K., and Sanderson, B. M.: The Scenario Model Intercomparison Project (ScenarioMIP) for CMIP6, Geoscientific Model Development, 9, 3461–3482, https://doi.org/10.5194/gmd-9-3461-2016, 2016.

Palter, J. B.: The Role of the Gulf Stream in European Climate, Annu. Rev. Mar. Sci., 7, 113–137, https://doi.org/10.1146/annurev-marine-010814-015656, 2015.

Peña-Molino, B. and Joyce, T. M.: Variability in the Slope Water and its relation to the Gulf Stream path, Geophys. Res. Lett., 35, L03606, https://doi.org/10.1029/2007GL032183, 2008.

Pérez-Hernández, M. D. and Joyce, T. M.: Two Modes of Gulf Stream Variability Revealed in the Last Two Decades of Satellite Altimeter Data, Journal of Physical Oceanography, 44, 149–163, https://doi.org/10.1175/JPO-D-13-0136.1, 2014.

Peterson, I., Greenan, B., Gilbert, D., and Hebert, D.: Variability and wind forcing of ocean temperature and thermal fronts in the Slope Water region of the Northwest Atlantic, J. Geophys. Res. Oceans, 122, 7325–7343, https://doi.org/10.1002/2017JC012788, 2017.

Rahmstorf, S., Box, J. E., Feulner, G., Mann, M. E., Robinson, A., Rutherford, S., and Schaffernicht, E. J.: Exceptional twentieth-century slowdown in Atlantic Ocean overturning circulation, Nature Clim Change, 5, 475–480, https://doi.org/10.1038/nclimate2554, 2015.

Reick, C. H., Raddatz, T., Brovkin, V., and Gayler, V.: Representation of natural and anthropogenic land cover change in MPI-ESM, Journal of Advances in Modeling Earth Systems, 5, 459–482, https://doi.org/10.1002/jame.20022, 2013.

Ross, A. C., Stock, C. A., Adcroft, A., Curchitser, E., Hallberg, R., Harrison, M. J., Hedstrom, K., Zadeh, N., Alexander, M., Chen, W., Drenkard, E. J., du Pontavice, H., Dussin, R., Gomez, F., John, J. G., Kang, D., Lavoie, D., Resplandy, L., Roobaert, A., Saba, V., Shin, S.-I., Siedlecki, S., and Simkins, J.: A high-resolution physical–biogeochemical model for marine resource applications in the northwest Atlantic (MOM6-COBALT-NWA12 v1.0), Geoscientific Model Development, 16, 6943–6985, https://doi.org/10.5194/gmd-16-6943-2023, 2023.

Rossby, T., Flagg, C. N., Donohue, K., Sanchez-Franks, A., and Lillibridge, J.: On the long-term stability of Gulf Stream transport based on 20 years of direct measurements, Geophysical Research Letters, 41, 114–120, https://doi.org/10.1002/2013GL058636, 2014.

Saba, V. S., Griffies, S. M., Anderson, W. G., Winton, M., Alexander, M. A., Delworth, T. L., Hare, J. A., Harrison, M. J., Rosati, A., Vecchi, G. A., and Zhang, R.: Enhanced warming of the Northwest Atlantic Ocean under climate change, J. Geophys. Res. Oceans, 121, 118–132, https://doi.org/10.1002/2015JC011346, 2016.

Sánchez-Román, A., Gues, F., Bourdalle-Badie, R., Pujol, M.-I., Pascual, A., and Drévillon, M.: Changes in the Gulf Stream path over the last 3 decades, State of the Planet, 4-osr8, 1–11, https://doi.org/10.5194/sp-4-osr8-4-2024, 2024.

Seidov, D., Mishonov, A., Reagan, J., and Parsons, R.: Resilience of the Gulf Stream path on decadal and longer timescales, Sci Rep, 9, 11549, https://doi.org/10.1038/s41598-019-48011-9, 2019.

Seidov, D., Mishonov, A., and Parsons, R.: Recent warming and decadal variability of Gulf of Maine and Slope Water, Limnology and Oceanography, 66, 3472–3488, https://doi.org/10.1002/lno.11892, 2021.

Taylor, A. H. and Stephens, J. A.: The North Atlantic Oscillation and the latitude of the Gulf Stream, Tellus A: Dynamic Meteorology and Oceanography, 50, 134–142, 1998.

Thompson, K. R. and Demirov, E.: Skewness of sea level variability of the world's oceans, Journal of Geophysical Research: Oceans, 111, https://doi.org/10.1029/2004JC002839, 2006.

Thornalley, D. J. R., Oppo, D. W., Ortega, P., Robson, J. I., Brierley, C. M., Davis, R., Hall, I. R., Moffa-Sanchez, P., Rose, N. L., Spooner, P. T., Yashayaev, I., and Keigwin, L. D.: Anomalously weak Labrador Sea convection and Atlantic overturning during the past 150 years, Nature, 556, 227–230, https://doi.org/10.1038/s41586-018-0007-4, 2018.

Todd, R. E. and Ren, A. S.: Warming and lateral shift of the Gulf Stream from in situ observations since 2001, Nat. Clim. Chang., 13, 1348–1352, https://doi.org/10.1038/s41558-023-01835-w, 2023.

Valcke, S.: The OASIS3 coupler: a European climate modelling community software, Geoscientific Model Development, 6, 373–388, https://doi.org/10.5194/gmd-6-373-2013, 2013.

Wenta, M., Grams, C. M., Papritz, L., and Federer, M.: Linking Gulf Stream air–sea interactions to the exceptional blocking episode in February 2019: a Lagrangian perspective, Weather and Climate Dynamics, 5, 181–209, https://doi.org/10.5194/wcd-5-181-2024, 2024.

Williams, R. G., Katavouta, A., and Roussenov, V.: Regional Asymmetries in Ocean Heat and Carbon Storage due to Dynamic Redistribution in Climate Model Projections, Journal of Climate, 34, 3907–3925, https://doi.org/10.1175/JCLI-D-20-0519.1, 2021.

Wu, T. and He, R.: Gulf Stream mesoscale variabilities drive bottom marine heatwaves in Northwest Atlantic continental margin methane seeps, Commun Earth Environ, 5, 1–12, https://doi.org/10.1038/s43247-024-01742-8, 2024.

Yang, H., Lohmann, G., Wei, W., Dima, M., Ionita, M., and Liu, J.: Intensification and poleward shift of subtropical western boundary currents in a warming climate, J. Geophys. Res. Oceans, 121, 4928–4945, https://doi.org/10.1002/2015JC011513, 2016.

Yang, H., Lohmann, G., Krebs-Kanzow, U., Ionita, M., Shi, X., Sidorenko, D., Gong, X., Chen, X., and Gowan, E. J.: Poleward Shift of the Major Ocean Gyres Detected in a Warming Climate, Geophysical Research Letters, 47, e2019GL085868, https://doi.org/10.1029/2019GL085868, 2020.